Heliosphere in the Local Interstellar Medium

Nikolai Pogorelov, University of Alabama in Huntsville, Huntsville, USA
Charles N. Arge, Goddard Space Flight Center, Greenbelt, MD, USA
Ratan Bera, University of Alabama in Huntsville, Huntsville, AL, USA
Leonard F. Burlaga, Leonard F. Burlaga, Inc., Davidsonville, MD 21035, USA
Federico Fraternale, University of Alabama in Huntsville, Huntsville, USA
Michael Gedalin, Ben-Gurion University of the Negev, Beer Sheva, Israel
Jacob Heerikhuisen, University of Waikato, New Zealand
Tae K. Kim, University of Alabama in Huntsville, Huntsville, USA
Jon Linker, Predictive Science Incorporated, San Diego, CA, USA
Vadim Roytershteyn, Space Research Institute, Boulder, CO, USA
Talwinder Singh, University of Alabama in Huntsville, Huntsville, USA
Lisa Upton, Southwest Research Institute, Boulder, CO, USA
Mehmet S. Yalim, University of Alabama in Huntsville, Huntsville, USA

Synopsis

The Sun moves with respect to the local interstellar medium (LISM) and modifies its properties to heliocentric distances as large as 1 pc. The solar wind (SW) is affected by penetration of the LISM neutral particles, especially H and He atoms. Charge exchange between the LISM atoms and SW ions creates pickup ions (PUIs) and secondary neutral atoms that can propagate deep into the LISM. Neutral atoms measured at 1 au can provide us with valuable information on the properties of pristine LISM. *New Horizons* provides us with unique measurements of pickup ions in the SW region where they are thermodynamically dominant. *Voyager* 1 and 2 spacecraft perform in-situ measurements of the LISM perturbed by the presence of the heliosphere and relate them to the unperturbed region. The *Interstellar Boundary Explorer* (*IBEX*) makes it possible identify the 3-D structure of the heliospheric interface. We outline the main challenges in the physics of the SW–LISM interaction. The physical processes that require a focused attention of the heliospheric community are discussed from the theoretical perspective and space missions necessary for their investigation. We emphasize the importance of data-driven simulations, which are necessary for the interpretation and explanation of spacecraft data.

1. Introduction

The interaction of the solar wind (SW) with the local interstellar medium (LISM) is a natural laboratory that allows the space physics and astrophysics communities to investigate a number of interesting physical phenomena in partially ionized plasma. Although the interaction of two plasma streams seems to be a trivial problem in the MHD sense, this is not so because the density of neutral hydrogen (H) atoms in the LISM surrounding the heliosphere is maybe three times higher than that of protons. While a tangential discontinuity, called the heliopause (HP), is formed in the ionized component, the interstellar neutral (ISN) atoms are able to penetrate deep into the heliosphere. The interaction of the ISN atoms with the SW ions occurs predominantly through the resonant charge exchange. As a result of such interaction, new neutral atoms are born with the properties of the parent SW ions and new ions with the properties of the parent ISN atoms. Newly born (secondary) neutral atoms and ions have properties strongly dependent on where in the heliosphere they were created. The flow of SW ions at distances exceeding 10-15 solar radii is super-fast magnetosonic, so its deceleration by the HP and LISM counter-pressure in the heliotail creates a heliospheric termination shock (TS). Thus, the secondary neutral atoms born inside the TS will be cool but have high radial velocity components. They make a so-called neutral SW. The secondary atoms born in the heliosheath (HS, the SW region between the TS and HP) are hot, but have low bulk speed. Because of the large charge-exchange mean free path, both populations of secondary neutral atoms can easily propagate back into the LISM and affect its properties to distances of 500-1000 AU in the upwind direction (Gruntman, 1982). Therefore, the pristine LISM becomes heated and decelerated by these secondary atoms via charge exchange. This is why, even if the LISM is superfast magnetosonic at very large distances, there may be no bow shock in the LISM in front of the HP (see Fig. 1), at least in certain radial directions. The presence of the heliosphere affects the LISM plasma to much larger distances in the heliotail region. Moreover, *ions of different energies are affected differently* (e.g., PeV galactic comic rays, GCRs, may be affected to distances of the order of 1 pc), which makes it difficult to establish the part of the LISM modified by the heliosphere exactly. It is for this reason, Fraternale & Pogorelov (2021) proposed to extend the term Very Local Interstellar Medium (VLISM) to the LISM affected by the presence of the heliosphere, regardless of what physical processes are responsible for such modification and which physical quantities are affected. The space filled by the VLISM between the HP and the bow shock/wave is sometimes called the outer heliosheath (OHS).

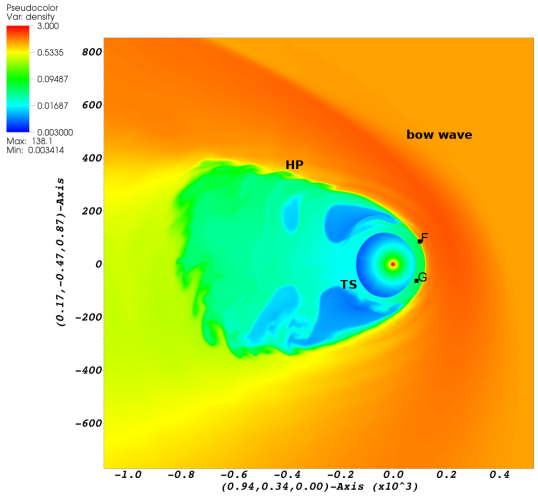

Figure 1: The picture of the SW–LISM interaction is shown through the plasma density distribution in the plane formed by the *V1* and *V2* trajectories. Letters F and G show the spacecraft positions in 2015. While the HP crossing distance at *V1* is closely reproduced, we also predicted that *V2* may cross the HP at a close distance. [From Pogorelov et al. (2015)]

The secondary ions born in the SW due to charge exchange are quickly isotropized, but never reach the state of thermodynamic equilibrium (Vasyliunas & Siscoe, 1976). These non-thermal ions are also called pickup ions (PUIs). They carry the majority of SW thermal energy starting from distances of the order of 10 AU and extending to the HP itself. We loosely distinguish the

inner and outer heliosphere (IH and OH) by assuming that the former starts at some critical, Sun-centered sphere with radial velocity component exceeding the fast magnetosonic speed and ends when the effect of PUIs on the SW flow becomes noticeable. The OH extends to the HP itself. Pickup protons co-move with the thermal protons in the direction of the HP (Parker, 1963). The effect of ion, especially PUI, streaming along magnetic field (**B**) lines cannot be excluded, but it is likely limited by scattering by turbulence. It is worthwhile to mention that the mere applicability of the MHD treatment of collisionless SW plasma relies upon such scattering. Since the thermal energy of PUIs is high and they can experience charge exchange themselves, newly born atoms are called energetic neutral atoms (ENAs). PUIs can also be born in the OHS behind the HP, where they ultimately give birth to new ENAs. Those ENAs which are born in the HS and OHS can propagate back to Earth, where they are measured by the *Interstellar Boundary Explorer* (McComas et al., 2017b), *Cassini*/INCA (Krimigis et al., 2009), and *Solar Heliospheric Observatory* (*SOHO*/HSTOF) (Hilchenbach et al., 1998; Czechowski et al., 2006). Since ENAs carry information about PUIs throughout the SW–LISM interaction region, they are used as a tool to describe the global structure of the heliosphere (Reisenfeld et al., 2021). This information is enhanced by in situ measurements performed by near-Earth spacecraft and *Voyager* 1 and 2, which crossed the TS and HP and are performing measurements in the VLISM (Stone et al., 2005, 2008, 2013, 2019). The more recent *New Horizons* (*NH*) mission is measuring the PUI and thermal SW properties at distances now exceeding 40 AU (McComas et al., 2017a), where PUIs are energetically dominant. *Interstellar Mapping Probe* (*IMAP*) is a new NASA mission, to be launched in 2024. It will perform ENA and PUI measurements with even higher accuracy (McComas et al., 2018). More details can be found in the review papers Bzowski et al. (2009); Izmodenov et al. (2009); Pogorelov et al. (2009, 2017b); Zank (1999); and Zank (2015).

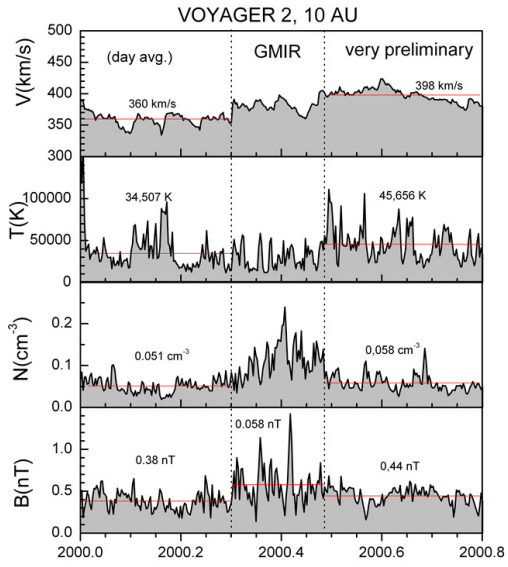

Figure 2: Quantity distributions in a typical GMIR observed by *V2*. The data is shifted by 234 days towards 10 AU.

The abundance of in-situ data and remote observations makes numerical simulations challenging. Their predictive power is strongly constrained by observations and mostly applies to the regions lacking in-situ measurements. For example, both *Voyagers* move into the nose of the SW–LISM interaction region. On the other hand, *IBEX* measurements of ENA fluxes are lacking those created at distances exceeding 500 AU into the heliotail. It is therefore virtually impossible to constrain the heliotail length and structure by data only. Although all numerical simulations based on identical models and physical boundary conditions give agreeable results, controversies are still possible on the border of model applicability. As far as in-situ measurements are concerned, they are performed at one point per time and remain therefore incomplete, as far as the global time-dependent picture is concerned.

In the following sections, a number of challenges are described that affect predictive capabilities of numerical modeling. Physical phenomena accompanying the SW–LISM interaction are so broad that many of them are applicable to various astrophysical objects.

2. Challenges in our understanding of the SW–LISM interaction

The challenges to be discussed can be separated into two categories. Firstly, it is important to choose a proper physical model. Secondly, any model should be accompanied by appropriate, typically time-dependent, boundary conditions. While ideal MHD models are commonly used to describe the SW and LISM plasma flow, the former is collisionless. The applicability of fluid equations is justified by ion scattering on magnetic field fluctuations abundant in the SW. On the other hand, p-H charge exchange mean free path is at least of the order of characteristic distances in the interaction region (e.g., the measured distance between the TS and HP is about 35 AU), so the transport of neutral atoms should be modeled kinetically (Baranov & Malama, 1993). This does not mean that simpler models, where different populations of neutral atoms are treated gas dynamically, cannot be used (see a comparison of these models in Pogorelov et al., 2009).

2.1 Data-driven boundary conditions

To simulate the SW behavior, it is necessary to identify a set of boundary conditions (b.c.'s). Remote observations of the solar magnetic field are made routinely in the photosphere. These data can be used as bb.c.'s for solar coronal models that propagate the SW beyond the critical sphere. In other words, solutions to the SW–LISM interaction can be driven and validated by data. To perform meaningful comparison with data at least the following observational issues should be addressed:

(1) Better shock identification algorithms to be developed especially for the HS data.

(2) A systematic search for the sectors and sector boundaries should be performed beyond the TS. Theoretical explanations should be provided for their presence and apparent occasional destruction possibly through local magnetic reconnection.

(3) SW and OHS observations should be used for theoretical studies of the formation of pressure fronts and their breaking.

(4) Relatively high-frequency, quasi-periodic structures have been observed in the HS and in the VLISM. Their nature and origin should be revealed.

(5) The SW, including the one in the HS, is a driven, open dynamical system, and the appropriate statistical mechanics is that of Tsallis (2009). The q-triplet seems to be a universal characteristic of the system. Since the Tsallis statistics is associated with the Lorentzian distribution suitable for the mixture of thermal ions and PUIs, much could be learned from this approach, particularly on relatively small scales.

(6) Many corotating interaction regions (CIRs), merged interaction regions (MIRs), and global MIRs (GMIRs, Fig. 2), associated with a decrease in the Galactic cosmic ray (GCR) intensity, have been observed in the HS. This is why, cosmic ray data should be involved in the data analysis.

(7) The question to be answered by combining observations and simulations is about why MIRs and GMIRs survive out to near the HP. In addition, no numerical model so far has been able to reproduce *V2* data in the HS satisfactorily. Models that extend from the Sun through the HS are suitable for addressing these questions.

Different coronal models constrained by remote and in situ SW observations (e.g. Arge et al., 2013; Caplan et al., 2021) allow us to create the b.c.'s at 20-25 solar radii. The inner b.c.'s for the ambient SW can be transferred with MHD simulations (Pogorelov et al., 2014) to the Earth's orbit with the uncertainty quantification (UQ). The properties of a selected few *Voyager*- and *NH*-directed coronal mass ejections (CMEs) are derived from publicly available remote observations made by *SDO* AIA and HMI, *STEREO* A & B COR2 and H1/H2, and *SOHO* C2/C3 instruments. An additional UQ analysis should performed of the solution dependence on the

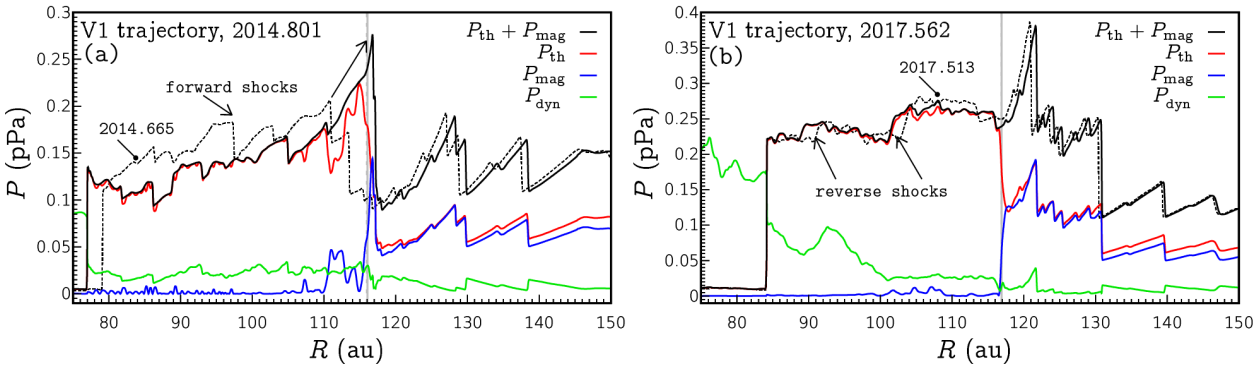

Figure 3: Two time frames with the pressure distributions along the *V1* trajectory show the forward and reverse shocks propagating through the HS. The dashed lines correspond to slightly shifted moments of time. One can also see shocks merging beyond the HP, the position of which is shown with vertical lines.

observationally-derived CME properties at injection sites. *Parker Solar Probe* (*PSP*), *OMNI*, and *Ulysses* (SWOOPS and SWICS) data can be used for validation in the IH. In the OH, Voyager (MAG and PLS) and *NH* SWAP data can be engaged.

If PUIs are treated as a separate fluid, the mixture of thermal and non-thermal ions in the SW can modeled in the assumption of different kappa distribution functions, which makes it possible, to perform a UQ based on this important parameter. The UQ analysis can be done on the basis of error propagation from 1 AU through the heliosphere.

Any fruitful research approach should be based on the historically proven idea that theory and numerical simulations are of immense importance for the interpretation of observational data. The latter, while providing us with the ground truth about the physical processes occurring in the heliosphere, highly benefit from the capability of modeling to experiment with the b.c.'s, switch on and off different processes, and provide global solutions. Such solutions are especially important if they are time-dependent and account for the realistic space dimensionality of the problem.

The b.c.'s in the unperturbed LISM are typically derived from the He atom measurements (McComas et al., 2015), especially those atoms that experience no charge exchange on the way to 1 AU. They give us the velocity components and temperature of the LISM. The prior estimates should be re-analyzed because the distribution function of pristine He atoms becomes anisotropic at 1 AU. (Wood et al., 2019; Swaczyna et al., 2020; Fraternale et al., 2021). The atom (H and He) and proton densities remain uncertain and are destined to be partially derived from the SW–LISM simulation results, especially for the He atom transport towards *IBEX* of *IMAP*.

In situ measurements are typically made at each individual point and time and therefore may hide the actual complexity of a phenomenon. As shown in Fig. 3a, the numerical simulation from Pogorelov et al. (2021) makes it possible not only to identify forward and reverse shocks in the HS, but also see their evolution in time. In addition, one can see overtaking of shocks propagating upstream in the LISM – the phenomenon so infrequent that it can hardly be observed by a single spacecraft.

Another surprising observation (Stone et al., 2008) was that *V2* crossed the TS at a much smaller heliocentric distance than *V1* (84 AU against 94 AU). While a number of possible explanation were proposed, some entirely unrealistic, the simulation of Pogorelov et al. (2013) driven by *Ulysses* measurement reproduced both the crossing time and the corresponding stand-off distances.

2.2. Pick up ions crossing the termination shock. The width of the heliosheath

Although the SW plasma consists of the thermal SW ions and PUIs, we choose to solve

the MHD system for the plasma mixture in the conservation-law form because this allows us to satisfy the conservation laws of mass, momentum, energy, and magnetic flux at the TS efficiently.

To address the behavior of PUIs in the heliosphere, it is essential to model them separately from the thermal SW. This can be done either by treating them kinetically or by solving additional fluid dynamics equations. Assuming that PUIs are isotropic away from discontinuities, simplifies the problem (Zank, 1999; Pogorelov et al., 2016). This is easier to implement in the supersonic SW inside the TS (Kim et al., 2016), see Fig. 4 that shows the comparison of simulations with *NH* observations. The effect of SW heating by turbulence produced by PUIs is also taken into account (Breech et al., 2008).

The description of PUIs crossing collisionless shocks, is impossible with the MHD, ideal or dissipative, approaches, because the details of kinetic shock structure are responsible for PUI reflections into the upstream region. Some kind of modified Rankine–Hugoniot-type boundary conditions describing the PUI transition across the TS are required. The fluid descriptions of the TS crossings by PUIs have been made so far either with simplified shock conditions (Pogorelov et al., 2016; Wu et al., 2016; Kornbleuth et al., 2020) or no conditions at all (Usmanov et al., 2016). Gedalin et al. (2020, 2021a,b) performed an extensive test-particle, full-PIC, nd hybrid simulations to derive such b.c.'s, but this research should be continued. Approaches as described above are essential to fit observational data in the IH. Besides, local kinetic simulations make it possible to describe the changes in the ion distribution function across the shock and apply the results to kinetic modeling of PUIs in the IH.

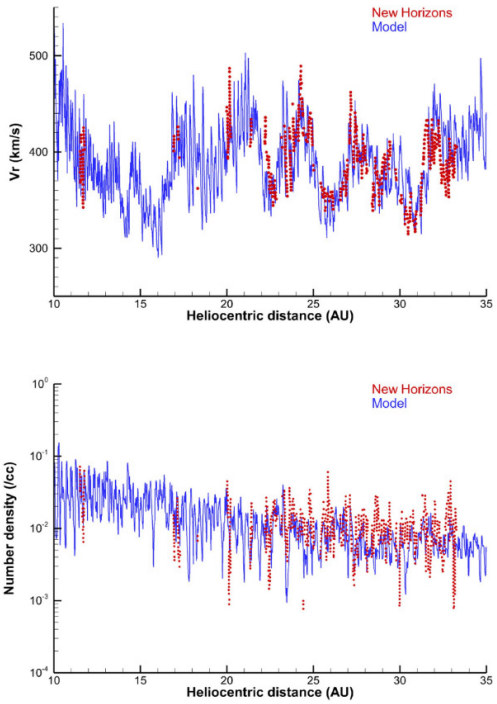

Figure 4: Radial velocity component and number density compared to the daily averaged *NH* SWAP data. [From Kim et al. (2016) with permission of the American Astronomical Society].

One of the improvements of the SW flow description in the IH would be the development of a turbulence model that would take care of both the Alfvénic and compressible components.

The discussion of the *HS width* is complicated by the absence of in situ measurements for the TS and HP distances from the Sun at the same moment of time. Pogorelov et al. (2015) predicted that *V2* should cross the HP at at a distance very close to that of *V1*. A separate treatment of PUIs indeed decreases the HS width (Pogorelov et al., 2016). However, data-driven numerical simulations reported by Kim et al. (2017) and Pogorelov et al. (2021), where PUIs were not treated separately, showed this width is variable: it has been smaller than 40 au since about 2014, reached 30 au in 2017, and now remains almost constant (about 35 au) in the *V1* direction. This is rather close to the difference between the observed crossings of the TS and HP. The IH width was consistently smaller in the *V2* direction, but they became almost identical starting 2017.

2.3 The effect of magnetic field dissipation on the thermodynamic properties and velocity of the SW in the IHS The HMF becomes almost radial at 0.1 au from the Sun. However, the regions of positive and negative polarity are separated by a current-carrying surface, which is called the heliospheric current sheet (HCS). Due to the Sun's rotation, the HMF lines acquire spiral shape.

However, the Sun's magnetic and rotation do not coincide, which creates the regions of opposite polarity. The width of each magnetic field sector decreases with decrease in the SW speed and vanishes near the SW stagnation point on the HP surface. While one would expect some sort of numerical dissipation of the HMF in this case, the simulated HMF strength starts to oscillate exhibiting the features of stochastic behavior (Pogorelov et al., 2015), if the grid resolution is sufficiently high. *Ulysses* data driven simulations presented by Pogorelov et al. (2013) show that the calculated value of the (dominant) transverse HMF component is of the order of 1 μG, which is close to the average value of the same, strongly oscillating component in observations. In principle, HMF dissipation should result in the SW heating and its slower deceleration. Identification of such features in the turbulent SW behind the TS is a challenging task, which is still to be undertaken.

An approach proposed by Czechowski et al. (2010) and Borovikov et al. (2011) was based on the idea that the HMF can be assumed unipolar in numerical simulations while the magnetic field polarity is assigned after each time step by tracing the HCS shape with a level-set method. However, this approach turned out to have two major deficiencies. Firstly, even the level-set equation sooner or later stops to resolve the sector structure. Secondly, the HMF strength becomes unrealistically strong (Izmodenov & Alexashov, 2020; Pogorelov et al., 2017a, 2021), which disagrees with *Voyager* data by a factor of ~ 7. Moreover, the plasma beta becomes less than 1 in the HS, so the SW flow gets under control of magnetic pressure, which can collimate the flow in the heliotail (Yu, 1974). The collimation occurs inside the Parker field branches spiraling into the tail region. In the extreme case of unipolar HMF, such spiraling can result into the heliotail splitting into two branches (Opher et al., 2015; Pogorelov et al., 2015). Such splitting disappears even in the assumption of a flat HCS, which happens when the Sun's magnetic and rotation axes coincide. Moreover, the reasons for the collimation disappear because of the "kinking" or "sausage" instabilities. Moreover, the solar cycle effects, especially the presence of the dense, slow and rarefied, fast SW regions with the variable latitudinal extent of the boundary between them completely destroys the artificial collimation, in this way removing the possibility of split-tail structures.

2.4. Magnetic field behavior in the VLISM

Pogorelov et al. (2021) show that time-dependent and data-driven numerical simulations can reproduce a surprising absence of the magnetic field rotation across the HP observed both by *V1* and *V2* (Burlaga et al., 2019). However, the actual reason for that remains unclear. This phenomenon cannot be universal, because the heliospheric magnetic field (HMF) polarity changes from cycle to cycle, while the interstellar magnetic field does not.

It is worth noting, however, that the behavior of magnetic field vectors across the HP along *V1* and *V2* trajectories cannot be reproduced with the boundary conditions assuming the unipolar HMF. The reasons are on the surface. As seen from Pogorelov et al. (2015, 2021); Izmodenov & Alexashov (2020), and Opher et al. (2020), B is practically continuous across the HP in the assumption of unipolar HMF. Since the HP is a tangential discontinuity, the equality of magnetic pressures across it can be satisfied only if the magnetic pressure dominates over the thermal pressure. This is in accord with our explanation of the exaggerated SW collimation inside the Parker field spirals bent into the heliotail.

2.5 Plasma wave generation in the VLISM and its relationship to the Alfvén velocity distributions along the Voyager trajectories newly derived from the spacecraft data

The subject discussed in the previous section is related with the distribution of the Alfvén velocity along the *V1* and *V2* trajectories in the VLISM. There is a close association between the electron plasma oscillations (Gurnett et al., 2013) and the jumps in the magnetic field strength

(Burlaga et al., 2013) observed in the OHS. According to PWS measurements (Gurnett et al., 2015), *V1* observed radio emission in the 2–3 kHz range, which is thought to be excited by shocks propagating through plasma regions primed with nonthermal electrons resonantly accelerated by lower hybrid (LH) waves driven by a ring-beam instability of PUIs (Gurnett et al., 1993; Cairns & Zank, 2002). Further acceleration of these electrons by a propagating shock may create electron beams moving away from it. The presence of nonthermal electrons is insufficient for the development LH instability. The instability growth rate and energy transfer to electrons should be sufficiently large, which occurs (see Cairns & Zank, 2002) if $\alpha_{\rm r} = V_{\rm r}/V_{\rm A} < 5$, where $V_{\rm r}$ and $V_{\rm A}$ are the PUI ring-beam and Alfvén velocities, respectively. Magnetic field draping around the HP creates conditions for larger $V_{\rm A}$. For PUIs born in the OHS by charge exchange of the VLISM ions with the neutral SW, which actually have a ring-beam distribution, $V_{\rm r}$ should be ~ 400 km/s.

Voyager data provide us with a new perspective on the plasma wave and radio emission generation. The analysis of these data in Pogorelov et al. (2021) showed that $V_{\rm A}$ decreases with distance from the HP, and is below 45 km/s at *V1* and 85 km/s at *V2* immediately after the HP. The Alfvénic velocity increases across the shocks traversing the OHS, but not substantially, since all shocks observed in that region so far have been rather weak. It is therefore unlikely that $\alpha_{\rm r}$ would be smaller than 5 for ring-beam velocities corresponding to the neutral SW. For this reason, a question remains on the physical mechanisms responsible for the plasma wave and radio emission generation on the OHS, since Roytershteyn et al. (2019) reported no substantial LH instability for a realistic, three-component distribution of PUIs beyond the HP.

It is essential to combine the observational data from *Voyager* with more detailed, kinetic simulations of plasma wave generation and radio emission at weakly collisional shocks. These phenomena are produced also by CME shocks in the inner heliosphere. This will make it possible to relate similar phenomena in very different plasma settings.

3. Spacecraft issues. This paper presented a number of observational phenomena that benefited from numerical simulations. Such simulations help understand in situ data obtained by an individual, or even two individual spacecraft, such as *V1* and *V2*. This is because one point in space per time observations may and do hide the details of stream and shock interaction. Of interest for large-scale simulations is the data analysis the VLISM turbulence performed by Fraternale & Pogorelov (2021). It was found, in particular, that the dissipative width of observed shock structures is too narrow to be attributed to Coulomb collisions alone. Moreover, high variability of the shock width structures suggests that that no actual shocks are observed in the collisional VLISM. Instead, *Voyagers* are crossed by sharp gradients which have not sufficient time to break in the turbulent plasma accompanied by transient wave activity.

Acnkowledgements: This work was supported in part by NASA grants 80NSSC20K1453, 80NSSC19K0260, 80NSSC18K1649, 80NSSC18K1212, AFOSR grant FA9550-19-1-0027, NSF-BSF grant PHY-2010450, and Hubble Space Telescope GO-15380.002-A. We separately acknowledge joint support from NSF (AGS-2028154) and NASA (80NSSC20K1582) within the Space Weather with Quantified Uncertainties program. Our work was also partially supported by the IBEX mission as a part of NASA's Explorer program. MG was partially supported by the EU Horizon2020 program under grant agreement No 101004131, and by NSF-BSF grant 2019744.
The authors acknowledges the Texas Advanced Computing Center (TACC) at The University of Texas at Austin for providing HPC resources on Frontera supported by NSF LRAC award 2031611. Supercomputing time allocations were also provided on SGI Pleiades by NASA High-End Computing Program award SMD-17-1537 and Stampede2 by NSF XSEDE project MCA07S033.

References

Arge, C. N., Henney, C. J., Hernandez, I. G., et al. 2013, in AIP Conference Series, Vol. 1539, Solar Wind 13, ed. G. P. Zank & et al., 11–14

Baranov, V. B., & Malama, Y. G. 1993, JGR, 98, 15157

Borovikov, S. N., Pogorelov, N. V., Burlaga, L. F., & Richardson, J. D. 2011, ApJL, 728, L21

Borovikov, S. N., Pogorelov, N. V., & Ebert, R. W. 2012, ApJ, 750, 42

Breech, B., Matthaeus, W. H., Minnie, J., Bieber, J. W., Oughton, S., Smith, C. W., & Isenberg, P. A. (2008), JGR, 113, 8105.

Burlaga, L., Ness, N. F., Berdichevsky, D., et al. 2019, Nature Ast., 3, 1007

Burlaga, L. F., Ness, N. F., Gurnett, D. A., & Kurth, W. S. 2013, ApJL, 778

Bzowski, M., Mobius, E., Tarnopolski, S., Izmodenov, V., & Gloeckler, G. 2009, SSR, 143, 177

Cairns, I. H. 1987, JGR, 92, 2329

Cairns, I. H., & Fuselier, S. A. 2017, ApJ, 834, 197

Cairns, I. H., & Zank, G. P. 2002, Geophys. Res. Lett., 29, 47

Caplan, R. M., Downs, C., Linker, J. A., & Mikic, Z. 2021, ApJ, 915, 44

Chalov, S. V., & Fahr, H. J. 2000, A&A, 360, 381

Colaninno, R. C., & Vourlidas, A. 2009, ApJ, 698, 852

Czechowski, A., Hilchenbach, M., Hsieh, K. C., Kallenbach, R., & Kóta, J. 2006, ApJL, 647, L69

Czechowski, A., Strumik, M., Grygorczuk, J., et al. 2010, A&A, 516, A17

DeStefano, A. M., & Heerikhuisen, J. 2017, in J. Phys. Conf. Ser., Vol. 837, 012013

DeStefano, A. M., & Heerikhuisen, J. 2020, Physics of Plasmas, 27, 032901

Dissauer, K., Veronig, A. M., Temmer, M., & Podladchikova, T. 2019, ApJ, 874, 123

Filbert, P. C., & Kellogg, P. J. 1979, JGR, 84, 1369

Fraternale, F., & Pogorelov, N. V. 2021, ApJ, 906, 75

Fraternale, F., Pogorelov, N. V., & Heerikhuisen, J. 2021, ApJL, 921, L24

Gedalin, M., Pogorelov, N. V., & Roytershteyn, V. 2020, ApJ, 889, 116

—. 2021a, ApJ, 910, 107

—. 2021b, ApJ, 916, 57

Gopalswamy, N., Akiyama, S., Yashiro, S., & Xie, H. 2018, JASTP, 180, 35

Gruntman, M. A. 1982, Soviet Astronomy Letters, 8, 24

Gurnett, D. A., Kurth, W. S., Allendorf, S. C., & Poynter, R. L. 1993, Science, 262, 199

Gurnett, D. A., Kurth, W. S., Burlaga, L. F., & Ness, N. F. 2013, Science, 341, 1489

Gurnett, D. A., Kurth, W. S., Stone, E. C., et al. 2015, ApJ, 809

Heerikhuisen, J., Zirnstein, E., & Pogorelov, N. 2015, JGR, 120, 1516

Heerikhuisen, J., Zirnstein, E. J., Pogorelov, N. V., Zank, G. P., & Desai, M. 2019, ApJ, 874, 76

Hilchenbach, M., Hsieh, K. C., Hovestadt, D., et al. 1998, ApJ, 503, 916

Isavnin, A. 2016, ApJ, 833, 267

Izmodenov, V. V., & Alexashov, D. B. 2020, A&A, 633, L12

Izmodenov, V. V., Malama, Y. G., Ruderman, M. S., et al. 2009, SSR, 146, 329

Kim, T. K., Pogorelov, N. V., & Burlaga, L. F. 2017, ApJL, 843

Kim, T. K., Pogorelov, N. V., Zank, G. P., Elliott, H. A., & McComas, D. J. 2016, ApJL, 832, 72

Kornbleuth, M., Opher, M., Michael, A. T., et al. 2020, ApJL, 895, L26

Krimigis, S. M., Mitchell, D. G., Roelof, E. C., Hsieh, K. C., & McComas, D. J. 2009, Science, 326, 971

Luoni, M. L., Démoulin, P., Mandrini, C. H., & van Driel-Gesztelyi, L. 2011, Solar Physics, 270, 45

McComas, D. J., Bzowski, M., Fuselier, S. A., et al. 2015, ApJS, 220, 22

McComas, D. J., Zirnstein, E. J., Bzowski, M., et al. 2017a, ApJS, 233, 8

—. 2017b, ApJS, 229, 41

McComas, D. J., Christian, E. R., Schwadron, N. A., et al. 2018, SSR, 214, 116

Opher, M., Drake, J. F., Zieger, B., & Gombosi, T. I. 2015, ApJL, 800

Opher, M., Loeb, A., Drake, J., & Toth, G. 2020, Nature Ast., 4, 675

Parker, E. N. 1963, Interplanetary dynamical processes (Interscience Publishers)

Pogorelov, N. V., Bedford, M. C., Kryukov, I. A., & Zank, G. P. 2016, J. Phys. Conf. Series, 767

Pogorelov, N. V., Borovikov, S., Heerikhuisen, J., et al. 2014, in Proc. 2014 Ann. Conf. on Extreme Science and Engineering Discovery Environment, XSEDE '14, 22:1–22:8

Pogorelov, N. V., Borovikov, S. N., Heerikhuisen, J., & Zhang, M. 2015, ApJL, 812

Pogorelov, N. V., Fraternale, F., Kim, T. K., Burlaga, L. F., & Gurnett, D. A. 2021, ApJ, 917, L20

Pogorelov, N. V., Heerikhuisen, J., Roytershteyn, V., et al. 2017a, ApJ, 845

Pogorelov, N. V., Heerikhuisen, J., Zank, G. P., & Borovikov, S. N. 2009, SSR, 143, 31

Pogorelov, N. V., Suess, S. T., Borovikov, S. N., et al. 2013, ApJ, 772

Pogorelov, N. V., Fichtner, H., Czechowski, A., et al. 2017b, SSR, 212, 193

Qiu, J., Hu, Q., Howard, T. A., & Yurchyshyn, V. B. 2007, ApJ, 659, 758

Reisenfeld, D. B., Bzowski, M., Funsten, H. O., et al. 2021, ApJS, 254, 40

Riley, P., Lionello, R., Caplan, R. M., et al. 2021, A&A, 650, A19

Roytershteyn, V., Pogorelov, N. V., & Heerikhuisen, J. 2019, ApJ, 881, 65

Schrijver, C. J., & De Rosa, M. L. 2003, Solar Physics, 212, 165

Singh, T., Kim, T. K., Pogorelov, N. V., & Arge, C. N. 2020a, Space Weather, 18, e02405

Singh, T., Yalim, M. S., Pogorelov, N. V., & Gopalswamy, N. 2019, ApJL, 875, L17

—. 2020b, ApJ, 894, 49

Steinolfson, R. S., Pizzo, V. J., & Holzer, T. 1994, Geophys. Res. Lett., 21, 245

Stone, E. C., Cummings, A. C., Heikkila, B. C., & Lal, N. 2019, Nature Ast., 3, 1013

Stone, E. C., Cummings, A. C., McDonald, F. B., et al. 2005, Science, 309, 2017

—. 2008, Nature, 454, 71

—. 2013, Science, 341, 150

Swaczyna, P., McComas, D. J., Zirnstein, E. J., et al. 2020, Astrophys. J., 903, 48

Thernisien, A., Vourlidas, A., & Howard, R. A. 2009, Solar Physics, 256, 111

Tsallis, C. 2009, Introduction to nonextensive statistical mechanics: approaching a complex world (Springer Science & Business Media)

Upton, L., & Hathaway, D. H. 2014, ApJ, 780, 5

Usmanov, A. V., Goldstein, M. L., & Matthaeus, W. H. 2016, ApJ, 820, 17

Vasyliunas, V. M., & Siscoe, G. L. 1976, JGR, 81, 1247

Wood, B. E., Müller, H.-R., & Möbius, E. 2019, ApJ, 881, 55

Wu, Y., Florinski, V., & Guo, X. 2016, ApJ, 832, 61

Yu, G. 1974, ApJ, 194, 187

Zank, G. P. 1999, SSR, 89, 413

—. 2015, ARAA, 53, 449

Zank, G. P., Heerikhuisen, J., Pogorelov, N. V., Burrows, R., & McComas, D. 2010, ApJ, 708, 1092